

## Extended X-Ray Absorption Fine Structure Measurements of Laser-Shocked V and Ti and Crystal Phase Transformation in Ti

B. Yaakobi, D. D. Meyerhofer, and T. R. Boehly

*Laboratory for Laser Energetics, University of Rochester, 250 East River Road, Rochester, New York 14623, USA*

J. J. Rehr

*Department of Physics, University of Washington, Seattle, Washington 98195, USA*

B. A. Remington, P. G. Allen, and S. M. Pollaine

*Lawrence Livermore National Laboratory, Livermore, California 94550, USA*

R. C. Albers

*Los Alamos National Laboratory, Los Alamos, New Mexico 87545, USA*

(Received 23 October 2003; published 5 March 2004)

Extended x-ray absorption fine structure (EXAFS), using a laser-imploded target as a source, can yield the properties of laser-shocked metals on a nanosecond time scale. EXAFS measurements of vanadium shocked to  $\sim 0.4$  Mbar yield the compression and temperature in good agreement with hydrodynamic simulations and shock-speed measurements. In laser-shocked titanium at the same pressure, the EXAFS modulation damping is much higher than is warranted by the predicted temperature increase. This is shown to be due to the  $\alpha$ -Ti to  $\omega$ -Ti crystal phase transformation, known to occur below  $\sim 0.1$  Mbar for slower shock waves.

DOI: 10.1103/PhysRevLett.92.095504

PACS numbers: 62.50.+p, 61.10.Ht, 61.80.Ba, 64.70.Kb

The dynamics of material response to shock loading has been extensively studied in the past [1]. The goal of those studies has been to understand the shock-induced deformation and structural changes at the microscopic level [2]. Laser-generated shocks can be employed to broaden these studies to higher pressures ( $\sim 1$  Mbar) and strain rates ( $\sim 10^7$ – $10^8$  s $^{-1}$ ). Recently, laser-shocked materials have been studied with *in situ* x-ray diffraction [3,4]. The goal of this work is to examine the use of *in situ* extended x-ray absorption fine structure (EXAFS) [5] as a complementary characterization of laser-shocked metals. EXAFS is the modulation in the x-ray absorption above the *K* edge (or *L* edge) due to the interference of the photoelectron waves with the waves reflected from neighboring atoms. The frequency of EXAFS modulations is related to the interparticle distance, hence to the compression. The damping rate of the modulation can yield the lattice temperature, *which is not readily available by other methods*.

*K*-edge EXAFS measurements were performed on vanadium and titanium shocked to  $\sim 0.5$  Mbar with a 3-ns laser pulse, provided by 3 of the 60 beams of the OMEGA laser [6]. The radiation source for the EXAFS measurement was obtained by imploding a spherical target using the remaining 57 beams. In a previous paper [7] we showed that a CH shell imploded by a multibeam laser system emits intense and spectrally smooth radiation, lasting  $\sim 120$  ps, suitable for EXAFS measurements. Figure 2(a) in Ref. [7] shows the smooth continuum spectrum from 4.5 to 7 keV, straddling the *K*-edge energy of Ti (4.96 keV) or of V (5.46 keV). For vanadium (where

no phase transformation exists below  $\sim 1$  Mbar) the measurements demonstrate that EXAFS is a useful method for measuring the compression and lattice temperature in  $\sim$ Mbar shocks. For Ti, where an  $\alpha$ -Ti to  $\omega$ -Ti crystal phase transformation is known to occur below  $\sim 0.1$  Mbar over microsecond time scales [8,9], the EXAFS measurements show that the transformation can occur over subnanosecond time scales.

This experiment constitutes a unique blend of solid-state physics, material science, and plasma physics. The EXAFS measurements, and particularly the diffraction measurements [3,4] of similar laser shocks, indicate that laser-shocked metals at pressures under  $\sim 1$  Mbar largely retain their crystal-order properties. On the other hand, the shock generation (in the laser-deposition region) as well as its propagation through the compressed metal was simulated with a plasma physics hydrodynamic code. The hydrodynamic code can simulate well the compressed solid because it incorporates a semiempirical equation of state [10] that is normalized to known experimental properties of the metal (such as specific heat, Grüneisen coefficient, and bulk modulus). The comparison of the code with experimental results forms the basis for the study of the compressed solid, which apart from its crystalline order constitutes also a high density, or strongly coupled plasma. Such plasmas are of great interest in understanding the interior of planets and the behavior of matter under extreme conditions.

Figure 1 shows a schematic of the target used to measure *K*-edge EXAFS spectra in laser-shocked targets. Flat-crystal spectrometer equipped with a Ge(1, 1, 1)

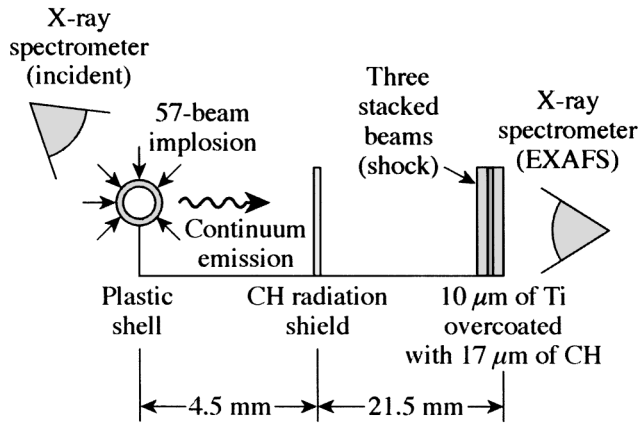


FIG. 1. Schematic of the experimental configuration. The imploding spherical target serves as a radiation source for EXAFS measurements. The three-stacked beams launch a shock through the Ti (or V) layer.

crystal was used for spectral dispersion. The three shock-generating laser beams were stacked to form a 3-ns-square pulse, focused to an irradiance of  $0.4$  to  $0.5$  TW/cm<sup>2</sup>. The delay time of the three-stacked beams with respect to the remaining beams was adjusted so that peak implosion (and emission) of the spherical target occurred when the shock wave exited the metal layer. The planar target consisted of  $10$ - $\mu$ m-thick polycrystalline V or Ti, coated on both sides with a  $17$ - $\mu$ m-thick CH. The heat shield ( $0.5$ -mm-thick CH foil) minimizes the heating of the metal layer due to soft radiation from the imploding spherical target. Although the EXAFS measurement is time integrated, a meaningful shock diagnosis can be obtained without streaking the spectrum in time because the x-ray pulse width is  $\sim 120$  ps [7], much shorter than the shock transit time through the metal ( $\sim 2$  ns).

The timing of the shock relative to the implosion-induced backlighter pulse was determined using the active shock breakout (ASBO) method, which uses a frequency-doubled yttrium aluminum garnet (YAG) laser probe, reflected from the backside of the target [11]. It also yields the shock speed in the metal, from which, using the known Hugoniot equation of state, the shock compression and pressure can be obtained. Finally, ASBO images indicate a lateral nonuniformity (due to the laser focal spot distribution) of  $\pm 10\%$  in the shock speed and, thus, also in the shock compression.

The expected shock strength and the properties of the shocked vanadium and titanium were determined using one-dimensional simulations with the hydrodynamic code LASNEX [12]. The range (around the volume average) of parameter values within the V layer is as follows: pressure,  $0.43 \pm 0.03$  Mbar; temperature,  $980 \pm 160$  K; volume compression,  $1.19 \pm 0.05$ . These variations in the axial direction are larger than the lateral variations due to laser nonuniformity; for this reason, a one-

dimensional simulation of the shocked metals is adequate. For Ti the comparable ranges are as follows: pressure,  $0.33 \pm 0.04$  Mbar; temperature,  $900 \pm 130$  K; volume compression,  $1.2 \pm 0.06$ . The EXAFS measurements average over the shocked volume.

The measured spectra were analyzed with the FEFF8 *ab initio* EXAFS software package [13]. The basic theory of EXAFS [5] yields an expression for the relative absorption  $\chi(k) = \mu(k)/\mu_0(k) - 1$ , where  $\mu(k)$  is the absorption coefficient and  $\mu_0(k)$  is the absorption of the isolated atom. The wave number  $k$  of the ejected photoelectron is given by the de Broglie relation  $\hbar^2 k^2 / 2m = E - E_K$ , where  $E$  is the absorbed photon energy and  $E_K$  is the energy of the  $K$  edge. FEFF8 uses the scattering potential to calculate the amplitude and phase shift of the photoelectron waves scattered from several shells of neighboring atoms including multiple-scattering paths. The total  $\chi(k)$  is constructed in the curved-wave approximation (i.e., the assumption of plane wave is removed) and iteratively fitted to the experimental  $\chi(k)$ . The main fitting parameters are the nearest-neighbor distance  $R$  and the vibration amplitude  $\sigma^2$  appearing in the Debye-Waller

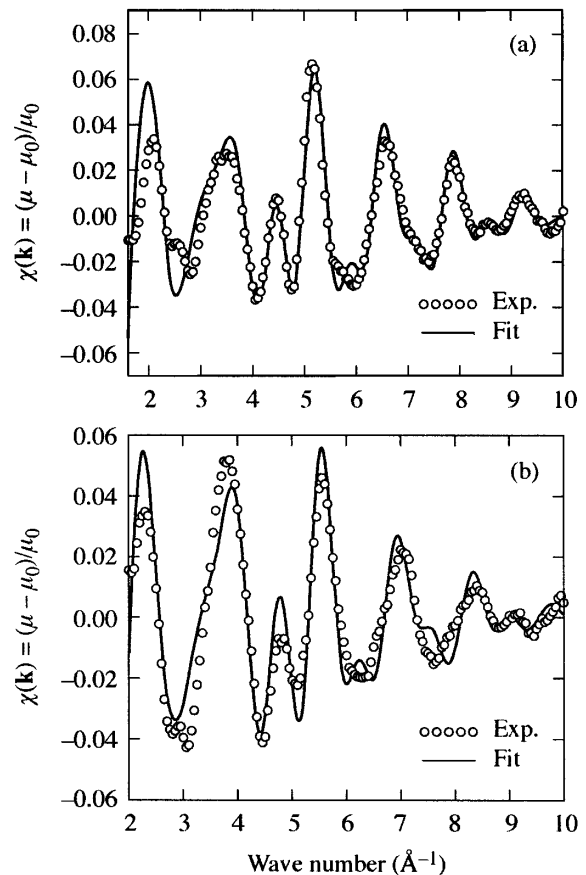


FIG. 2. Fitting the measured V EXAFS spectra for the unshocked case (a) and the shocked case (b) with the FEFF8 code, which allows for multiple electron scattering. The fitting parameters are detailed in the text.

TABLE I. Calculated and measured parameters for shocked vanadium. Laser intensity of  $0.5 \text{ TW/cm}^2$  yielding a pressure of  $\sim 0.45 \text{ Mbar}$ .

LASNEX Parameter ranges		EXAFS Measurement		Shock-speed Measurement
Compression	Temperature	Compression	Temperature	Compression
$1.19 \pm 0.05$	$980 \pm 160 \text{ K}$	$1.15 \pm 0.01$	$770 \pm 70 \text{ K}$	$1.15 \pm 0.06$

term.  $R$  yields the density or compression if we assume three-dimensional compression. The agreement of the resulting compression with the value derived from the shock-speed measurement justifies this assumption. The vibration amplitude  $\sigma^2$  depends mainly on the temperature but also on the compression.  $\sigma^2$  as a function of temperature is calculated using the Debye model [14] for the phonon density of states, including correlation between the motions of the absorbing and neighboring atoms.  $\sigma^2$  depends on the density through the Debye temperature. The density dependence of the Debye temperature was calculated using an empirical model [10]. Knowing the compression and  $\sigma^2$ , the temperature can be derived.

The results of fitting the V EXAFS spectra with the FEFF8 code are shown in Fig. 2(a) for the unshocked case and in Fig. 2(b) for the shocked case. For the unshocked case, the fitting parameters were (for the first-shell)  $R = (2.584 + 0.008) \text{ \AA}$  and  $\sigma^2 = (0.0111 \pm 0.0006) \text{ \AA}^2$ , yielding the temperature  $430 \pm 25 \text{ K}$ . The increase of  $\sim 130 \text{ K}$  over room temperature is due to residual radiation heating caused by the imploding target. For the shocked case, the fitting parameters (for the first shell) were  $R = (2.470 \pm 0.013) \text{ \AA}$  and  $\sigma^2 = (0.0147 \pm 0.0011) \text{ \AA}^2$ . Comparing  $R$  for the unshocked and shocked cases, we derive a volume compression of  $\sim 1.15$ . The resulting temperature is  $900 \pm 70 \text{ K}$ . This increase in temperature includes the effect of radiation heating. The net temperature due to the shock alone is  $770 \pm 70 \text{ K}$ .

Table I summarizes the measured and computed parameters for the shocked-V experiment. EXAFS results indicate a slightly weaker shock than predicted by LASNEX, but they are in agreement with the shock-speed measurement (as seen by the compression values). The measured values are accompanied by their uncertainties, whereas the LASNEX values are accompanied by their ranges in the axial direction.

Shocked titanium (in gas-gun experiments) is known to undergo an  $\alpha$ -Ti to  $\omega$ -Ti crystal phase transformation at a pressure in the range 0.029 to 0.09 Mbar, depending on sample purity [8,9]. The pressure in this experiment is well above this range, however, it was not known whether the transformation could occur on the nanosecond time scale of this experiment.

Figure 3(a) shows the fitting of the FEFF8 EXAFS code to the measured Ti EXAFS, taken at  $0.4 \text{ TW/cm}^2$ . Assuming the  $\alpha$ -Ti phase in the FEFF8 simulations, the

first-shell fitting parameters result in a volume compression of  $1.2 \pm 0.03$ . This compares well with the LASNEX value of  $1.2 \pm 0.06$ , but the error is much larger than for vanadium. However, the deduced  $\sigma^2$  value,  $0.029 \pm 0.008 \text{ \AA}^2$ , corresponds to a temperature of  $T = 2100 \pm 570 \text{ K}$ , in sharp disagreement with the LASNEX-predicted value ( $\sim 900 \text{ K}$ ). This strongly suggests that the large  $\sigma^2$  value is not due to a high temperature but due to a phase transformation. In fact, whereas each  $\alpha$ -Ti atom has six equidistant neighbors,  $\omega$ -Ti atoms have two possible atomic environments [8]: at site A there are 14 neighbors at two different distances, and at site B there are 11 neighbors at three different distances. Different distances translate to different EXAFS frequencies that, through beating, cause enhanced damping. Figure 3(b) shows this

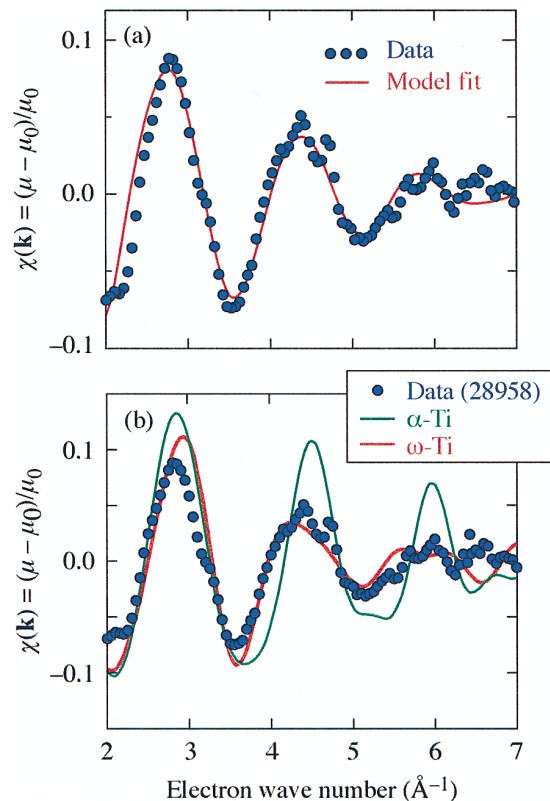


FIG. 3 (color). Fitting the FEFF8 EXAFS code to the measured Ti EXAFS spectrum (a) assuming the  $\alpha$ -Ti phase (the hcp phase at normal conditions) and adjusting the compression and damping rate. (b) assuming the  $\alpha$ -Ti phase and the  $\omega$ -Ti phase at  $T = 900 \text{ K}$  and adjusting only the compression.

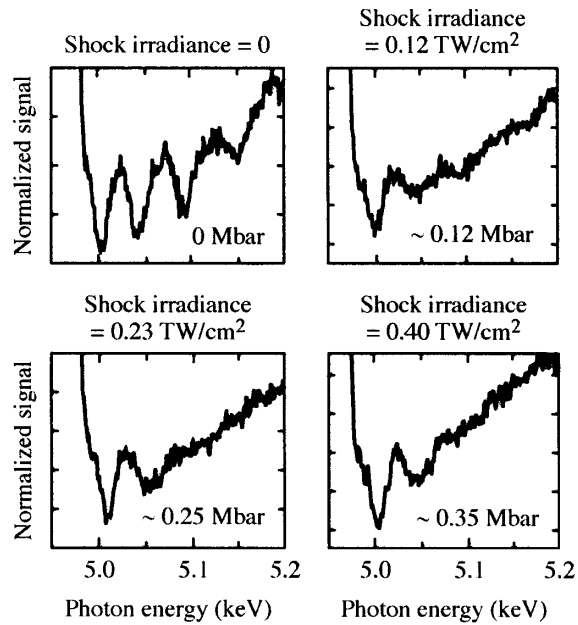


FIG. 4. Transmitted intensity from Ti for different values of the laser intensity (average pressure values from LASNEX are shown). A phase transformation at  $\sim 0.12$  Mbar is indicated.

to be the case. Here FEFF8 calculations assuming the  $\omega$ -Ti crystal structure, averaging over sites *A* and *B*, were carried out for the LASNEX-predicted temperature of 900 K. Only the compression was adjusted to fit the measured EXAFS frequency, and the resulting value of 1.23 is close to the predicted value of 1.2. It should be noted that the  $\alpha$ -Ti to  $\omega$ -Ti phase transformation entails an  $\sim 2\%$  volume compression [9]. Figure 3(b) clearly shows that assuming the  $\omega$ -Ti phase agrees with the experiment much better than assuming the  $\alpha$ -Ti phase. Thus, the damping is dominated by the crystal structure of  $\omega$ -Ti rather than by the temperature.

A critical test of the assumption of phase transformation can be obtained by repeating the measurement for successively weaker shocks. Figure 4 shows the transmitted x-ray intensity for four values of the laser intensity (volume-averaged pressures from LASNEX are indicated). The reduction of the intensity by a factor of  $\sim 2$  to  $0.23 \text{ TW/cm}^2$  shows no significant change in the spectrum. This strongly suggests that the high damping rate is not due to a high temperature. At an intensity of  $0.12 \text{ TW/cm}^2$  (corresponding to a shock pressure of

$\sim 0.12$  Mbar), the damping rate is intermediate between the shocked and the unshocked cases. This is consistent with a phase transformation occurring, very roughly, around 0.12 Mbar.

We therefore conclude that the observed high damping rate in shocked Ti is due to the  $\alpha$ -Ti to  $\omega$ -Ti phase transformation. In summary, *in situ* EXAFS using laser-imploded target as a radiation source has been shown to be a useful method for measuring compression and temperature in nanosecond-scale shocked metals and in studying shock-induced phase transformations.

The pole figures obtained by Professor S. Burns are gratefully acknowledged. This work was supported by the U.S. Department of Energy Office of Inertial Confinement Fusion under Cooperative Agreement No. DE-FC03-92SF1931,460, the University of Rochester, and the New York State Energy Research and Development Authority. The support of DOE does not constitute an endorsement by DOE of the views expressed in this Letter.

- 
- [1] C. A. Hall *et al.*, in *Shock Compression of Condensed Matter-1999*, edited by M. D. Furnish, L. C. Chhabildas, and R. S. Hixson (AIP, New York, 2000), pp. 1171–1174.
  - [2] Y. M. Gupta, in *Shock Compression of Condensed Matter*, edited by S. C. Schmidt, R. D. Dick, J. W. Forbes, and D. G. Tasker (North-Holland, Amsterdam, 1992), p. 15.
  - [3] D. H. Kalantar *et al.*, Phys. Plasmas **7**, 1999 (2000); D. H. Kalantar *et al.*, Phys. Plasmas **10**, 1569 (2003).
  - [4] L. Loveridge-Smith *et al.*, Phys. Rev. Lett. **86**, 2349 (2001).
  - [5] P. A. Lee *et al.*, Rev. Mod. Phys. **53**, 769 (1981).
  - [6] T. R. Boehly *et al.*, Rev. Sci. Instrum. **66**, 508 (1995).
  - [7] B. Yaakobi *et al.*, J. Opt. Soc. Am. B **20**, 238 (2003).
  - [8] S. K. Sikka, Y. K. Vohra, and R. Chidambaram, Prog. Mater. Sci. **27**, 245 (1982).
  - [9] C. W. Greeff, D. R. Trinkle, and R. C. Albers, J. Appl. Phys. **90**, 2221 (2001).
  - [10] R. M. More *et al.*, Phys. Fluids **31**, 3059 (1988).
  - [11] P. M. Celliers *et al.*, Appl. Phys. Lett. **73**, 1320 (1998).
  - [12] G. B. Zimmerman and W. L. Kruer, Comments Plasma Phys. Controlled Fusion **2**, 51 (1975).
  - [13] J. J. Rehr, R. C. Albers, and S. I. Zabinsky, Phys. Rev. Lett. **69**, 3397 (1992).
  - [14] E. Seviliano, H. Meuth, and J. J. Rehr, Phys. Rev. B **20**, 4908 (1979).